STAR Protocols

CellPress
OPEN ACCESS

Protocol

Immunofluorescence microscopy-based assessment of cytosolic DNA accumulation in mammalian cells

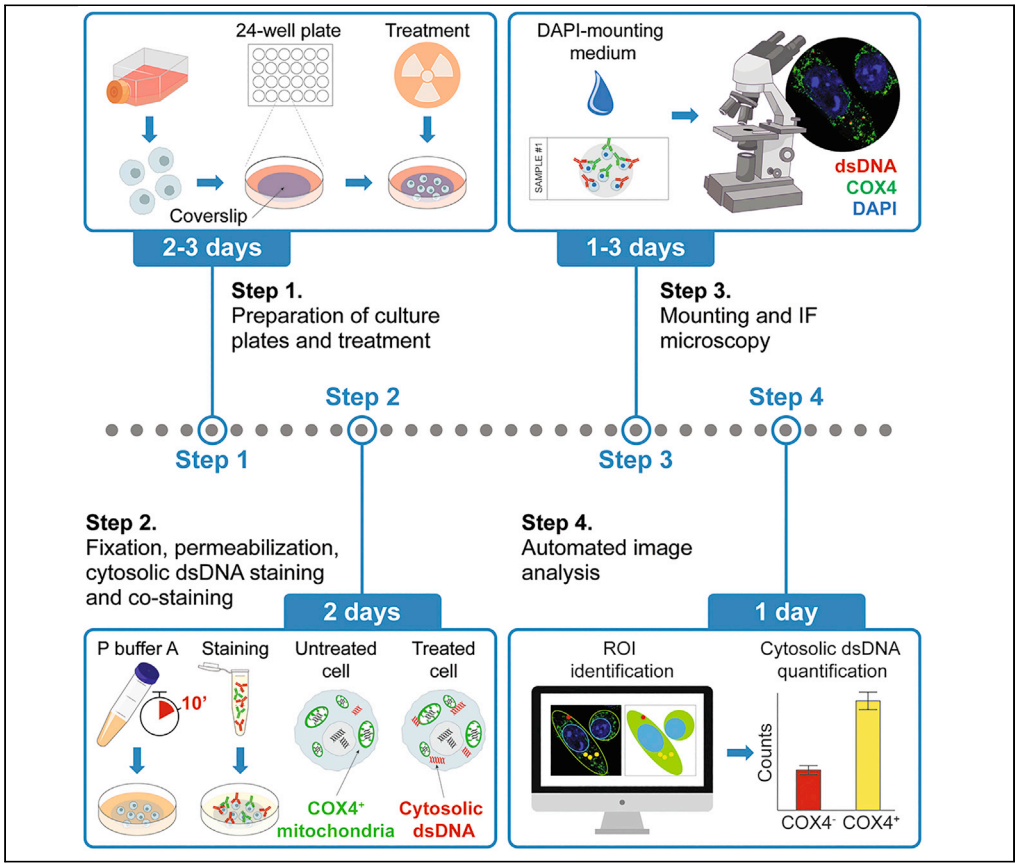

Here, we describe an immunofluorescence (IF) microscopy-based approach to quantify cytosolic double-stranded DNA molecules in cultured eukaryotic cells upon the selective and specific permeabilization of plasma membranes. This technique is compatible with widefield microscopy coupled with automated image analysis for mid- to high-throughput applications, and high-resolution confocal microscopy for subcellular assessments and co-localization studies. In addition to enabling single-cell and subcellular resolution, this approach circumvents most constraints associated with alternative approaches based on subcellular fractionation.

Ai Sato, Aitziber Buque, Takahiro Yamazaki, Norma Bloy, Giulia Petroni, Lorenzo Galluzzi

ais2010@med.cornell.edu (A.S.)
deadoc80@gmail.com (L.G.)

Highlights

Highly controlled permeabilization enables specific detection of cytosolic dsDNA

Compatible with co-staining for the co-detection of organellar markers

Amenable to confocal microscopy for high-resolution spatial assessments

Amenable to widefield microscopy and automated image analysis for quantitation

Sato et al., STAR Protocols 2, 100488
June 18, 2021
https://doi.org/10.1016/j.xpro.2021.100488

STAR Protocols

CellPress
OPEN ACCESS

Protocol

Immunofluorescence microscopy-based assessment of cytosolic DNA accumulation in mammalian cells

Ai Sato,[1,6,*] Aitziber Buque,[1] Takahiro Yamazaki,[1] Norma Bloy,[1] Giulia Petroni,[1] and Lorenzo Galluzzi[1,2,3,4,5,7,*]

[1]Department of Radiation Oncology, Weill Cornell Medical College, New York, NY 10065, USA

[2]Sandra and Edward Meyer Cancer Center, Weill Cornell Medical College, New York, NY 10065, USA

[3]Isreal and Caryl Englander Institute for Precision Medicine, Weill Cornell Medical College, New York, NY 10065, USA

[4]Department of Dermatology, Yale School of Medicine, New Haven, CT 06510, USA

[5]Université de Paris, Paris 75006, France

[6]Technical contact

[7]Lead contact

*Correspondence: ais2010@med.cornell.edu (A.S.), deadoc80@gmail.com (L.G.)
https://doi.org/10.1016/j.xpro.2021.100488

SUMMARY

Here, we describe an immunofluorescence (IF) microscopy-based approach to quantify cytosolic double-stranded DNA molecules in cultured eukaryotic cells upon the selective and specific permeabilization of plasma membranes. This technique is compatible with widefield microscopy coupled with automated image analysis for mid- to high-throughput applications and high-resolution confocal microscopy for subcellular assessments and co-localization studies. In addition to enabling single-cell and subcellular resolution, this approach circumvents most constraints associated with alternative approaches based on subcellular fractionation.

For complete use and execution of this protocol, please refer to Yamazaki et al. (2020).

BEFORE YOU BEGIN

The protocol below describes the specific steps for the immunofluorescence microscopy (IF)-assisted assessment and quantification of double-stranded DNA (dsDNA) molecules in the cytosol of mouse mammary adenocarcinoma TS/A cells (De Giovanni et al., 2019) maintained *in vitro* and optionally exposed to ionizing irradiation as a strategy to induce apoptotic mitochondrial outer membrane permeabilization (MOMP) coupled to mitochondrial DNA (mtDNA) release (Rodriguez-Ruiz et al., 2019; Rodriguez-Ruiz et al., 2020; Yamazaki et al., 2020). Specifically, the protocol offers a means to (1) quantify the number of cytosolic dsDNA-positive foci per cell; (2) quantify the percentage of cells containing a number of cytosolic dsDNA-positive foci higher than a predetermined threshold; and (3) qualitatively and quantitatively assess the spatial localization of cytosolic dsDNA-positive foci with respect to the nuclear marker lamin B1 (LMNB1), the mitochondrial marker cytochrome c oxidase subunit 4I1 (COX4I1, a component of the respiratory holo-enzyme commonly known as cytochrome c oxidase 4, COX4), and the mitochondrial transcription factor transcription factor A, mitochondrial (TFAM). Variations of this protocol have successfully been applied to numerous human and mouse cells subjected to a panel of experimental challenges *in vitro* (Lam et al., 2014; Shen et al., 2015; Vanpouille-Box et al., 2017a). Moreover, we expect this protocol to be suitable for qualitatively and quantitatively assessing the spatial localization of cytosolic dsDNA-positive foci with respect to cellular markers other than LMNB1, COX4 and TFAM, provided that such markers are not secluded within membranous compartments that do not get permeabilized by the procedures described herein. Previous work based on rather non-selective fixation and

permeabilization conditions, indeed, evidenced the co-localization of cytosolic dsDNA species and their sensor cyclic GMP-AMP synthase (CGAS) (Han et al., 2020; Vanpouille-Box et al., 2019).

Solutions are prepared following the recipes in the materials and equipment section. Solutions which are prepared in advance and can be stored are indicated. A complete list of materials and equipment required is given in the key resources table.

Preparation of cell culture plates

Timing: < 10 min per plate

⚠ CRITICAL: Cell culture plates should be prepared under a Class II Biological Safety Cabinet to minimize contaminations, even though a sterilization step is included for coverslips

⚠ CRITICAL: Coverslips are necessary for mounting stained samples on microscope slides.

1. Sterilize glass coverslips with 200 µL sterilization buffer for 2 min and deposit them in each well of 24-well plates

Note: We recommend the use of No. 1.5 coverslips as most objectives are corrected for optical aberrations with the assumption that this coverslip thickness is employed.

Alternatives: Coverslip sterilization can be achieved by autoclaving.

2. Rinse wells with 200 µL sterile PBS
3. Remove PBS

Note: The number of plates to be prepared with coverslips for cell culture depend on the number of experimental conditions to be tested, the number of stainings to be performed and potential limitations imposed by the experimental setup (example, many experimental irradiators do not enable the irradiation of specific wells). That said, at least 3 different wells should be used for each condition to enable triplicate intra-experiment assessments.

Pause point: Coverslip-containing plates can be stored at 20°C–25°C until use, although caution should be used to avoid contamination

KEY RESOURCES TABLE

REAGENT or RESOURCE	SOURCE	IDENTIFIER
Antibodies		
dsDNA antibody [HYB331-01]	Abcam	Cat# ab27156, RRID:AB_470907
Lamin B1 antibody - Nuclear Envelope Marker	Abcam	Cat# ab16048, RRID:AB_10107828
Rabbit Anti-COX IV - Mitochondrial Loading Control Polyclonal Antibody, Unconjugated	Abcam	Cat# ab16056, RRID:AB_443304
mtTFA antibody	GeneTex	Cat# GTX103231, RRID:AB_11176720
Goat Anti-Mouse IgG H&L (Alexa Fluor® 594) preadsorbed antibody	Abcam	Cat# ab150120, RRID:AB_2631447
Goat Anti-Rabbit IgG (H+L) Antibody, Alexa Fluor® 488 Conjugated	Thermo Fisher Scientific	Cat# A-11008, RRID:AB_143165
Chemicals, peptides, and recombinant proteins		
Tween-20	Sigma	Cat# P-1379
TritonX-100	Fisher Scientific	Cat# BP151-100

(*Continued on next page*)

Continued

REAGENT or RESOURCE	SOURCE	IDENTIFIER
Bovine Serum Albumin (BSA), Fraction V	Gemini Bio	Cat# 700-100P
PBS	Life Technologies	Cat# 10010023
4% PFA	Santa Cruz	Cat# sc-281692
ProLong Diamond Antifade Mountant with DAPI	Fisher Scientific	Cat# P36962
Dulbecco's modified Eagle's medium (DMEM), 4.5 g/L glucose	Corning	Cat# 15-017-CV
Foundation™ Fetal Bovine Serum	Gemini Bio	Cat# 900-108
HEPES (1 M)	Life Technologies	Cat# 15630-080
Penicillin-streptomycin-glutamine (100×)	Life Technologies	Cat# 10378016
Gentamicin (50 mg/mL)	Life Technologies	Cat# 15750078
2-Mercaptoethanol (55 mM)	Life Technologies	Cat# 21985023
Trypsin-EDTA solution	Sigma	Cat# T3924
Experimental models: cell lines		
TS/A mouse mammary adenocarcinoma cells	Millipore	Cat# SCC177
Software and algorithms		
CellProfiler	Broad Institute	RRID:SCR_007358
EVOS control software v. 1.4 (Rev 26059)	Thermo Fisher	N/A
ImageJ/Fiji	NIH	RRID:SCR_002285
Photoshop	Adobe	RRID:SCR_014199
SARRP control software, v. 4.3.1	Xstrahl	N/A
ZEN Black v. 2.3 SP1	Zeiss	RRID:SCR_018163
Other		
24-Well plates	Corning	Cat# 353226
Cover glasses (#1.5, 12 mm diameter)	Neuvitro	Cat# GG-12–1.5-oz
EVOS® FL Imaging System	Thermo Scientific	Cat# AMC1000
Graefe forceps	Fine Science Tools	Cat# 11650-10
Humidified chamber	Ted Pella	Cat# 2102
ImmEdge® Hydrophobic Barrier PAP Pen	Vector Laboratories	Cat# H-4000
LSM 880 confocal laser scanning microscope	Zeiss	RRID:SCR_020925
Microscope Slides, Diamond White Glass, 25 × 75 mm, Charged, 90° Ground Edges, Aqua Frosted	Thomas Scientific	Cat# 1184X34
Small Animal Radiation Research Platform (SARRP)	Xstrahl	N/A
T75 flasks	Thermo Scientific	Cat# 156499

MATERIALS AND EQUIPMENT

Equipment

- Milli-Q Water - Ultrapure Water System (Millipore) or equivalent system for ddH_2O purification
- Class II Biological Safety Cabinet
- CO_2 incubator for cell culture
- Cold room or refrigerator
- Humidified chamber
- Graefe forceps
- ImmEdge® Hydrophobic Barrier PAP Pen
- Widefield microscope or imager equipped with a Plan Fluorite 40×/0.65 objective, and LED/filter sets to acquire DAPI (excitation/emission peaks at ~358/461 nm respectively), Alexa Fluor® 488 (excitation/emission peaks at ~494/517 nm respectively) and Alexa Fluor® 594 (excitation/emission peaks at ~590/617 nm respectively) signals, such as the EVOS® FL Imaging System operated by embedded Software v. 1.4 (Rev 26059) (Thermo Fisher) employed here. Optical configuration:
  - Blue channel: 344–357 nm excitation with DAPI 2.0 LED light cube; 447–460 nm detection
  - Green channel: 482–525 nm excitation with GFP 2.0 LED light cube; 524 nm detection
  - Red channel: 529–585 nm excitation with Texas Red 2.0 LED light cube; 628–632 nm detection.

- Confocal microscope equipped with a Plan-Apochromat 63×/1.4 Oil DIC objective, and with laser/filter sets to acquire DAPI, Alexa Fluor® 488 and Alexa Fluor® 594 signals, such as the LSM 880 Confocal Laser Scanning Microscope operated by ZEN Black v. 2.3 SP1 (Zeiss) employed here. Optical configuration:
  - o Blue channel: 405 nm excitation with diode laser; 415–478 nm detection with PMT for short-wavelength dyes (Ch1)
  - o Green channel: 488 nm excitation with Argon laser; 498–555 nm detection with the GaAsP (Gallium) Arsenide Phosphide PMT - Airyscan detector for intermediate- wavelength dyes (Ch2)
  - o Red channel: 594 nm excitation with HeNe594 laser; 601–680 nm detection with PMT for long-wavelength dyes (Ch3)

Optional: autoclave

Optional: for irradiation studies, as the ones described herein, an irradiation platform that offers control on total dose, such as the Small Animal Radiation Research Platform (SARRP) operated by the SARRP Control Software, v. 4.3.1 (Xstrahl Medical & Life Sciences)

Solutions for TS/A cell culture

Timing: < 30 min

⚠ CRITICAL: All solutions employed for cell culture need to be prepared and maintained in sterile conditions by operating under a Class II Biological Safety Cabinet

- Complete medium for TS/A cell culture is prepared by adding the supplements specified in the table below to Dulbecco's Modified Eagle Medium (DMEM):

Component	Final concentration	Amount
Fetal bovine serum (FBS)	~10% v/v	55 mL
Penicillin-Streptomycin-Glutamine	~100 U/mL (penicillin) ~100 µg/mL (streptomycin) ~0.3 mg/mL (glutamine)	5.5 mL
Gentamicin	~50 µg/mL	0.55 mL
HEPES	~5 mM	2.75 mL
2-Mercaptoethanol	~50 µM	495 µL
DMEM basal medium	n/a	500 mL
Total	**n/a**	**~564 mL**

Note: Optimal medium composition can vary considerably for different cell types.

Note: Complete culture medium can be stored at 4° C for at least 1 month.

Note: Although FBS is classified as non-hazardous (NONH), it should be manipulated by wearing appropriate recommended personal protective equipment (PPE).

⚠ CRITICAL: Penicillin/Streptomycin may cause an allergic skin reaction (H317), may cause allergy or asthma symptoms or breathing difficulties if inhaled (H334), and may damage fertility or the unborn child (H360), and hence it should be manipulated by wearing appropriate recommended PPE.

- The sterilization buffer is prepared by mixing 700 mL of ethanol with 300 mL of distilled water.

⚠ CRITICAL: Ethanol is highly flammable in liquid and vapor (H225) and causes serious eye irritation (H319), and hence it should be manipulated by wearing appropriate recommended PPE and at distance from open flames, as well as potential sources of heat and sparkles, and it should be stored in dedicated cabinets for flammables.

Solutions for IF microscopy

Timing: < 1 h

- The bovine serum albumin (BSA) stock solution is prepared by diluting 2.5 *g* BSA in 50 mL PBS.
- Upon complete dissolution, the stock can be aliquoted in 2 mL and stored at −20°C for at least one year

Note: Although BSA is classified as non-hazardous (NONH), they should be manipulated by wearing appropriate recommended PPE.

- Tween20 and TritonX-100 stock solutions are prepared by diluting 1 mL Tween20 or TritonX-100 in 9 mL PBS, respectively, and allowing complete dissolution on a rocker for 30 min at 20°C–25°C

⚠ CRITICAL: Tween20 and TritonX-100 stock solutions are key to ensure accuracy and reproducibility in the composition of permeabilization buffers.

⚠ CRITICAL: TritonX-100 is classified as harmful if swallowed (H302), may cause skin irritation (H315), and causes serious eye damage (H318), and hence should be manipulated by wearing appropriate recommended PPE.

Note: Although Tween 20 is classified as NONH, they should be manipulated by wearing appropriate recommended PPE.

Note: Tween20 and TritonX-100 stock solutions are stable at 20°C–25 °C for at least one month.

- Permeabilization, blocking and washing buffers for IF microscopy are prepared as specified in the table below:

Permeabilization buffer A	Stock concentration	Final concentration	Amount
Tween 20	10% v/v	0.1% v/v	100 µL
TritonX-100	10% v/v	0.01% v/v	10 µL
PBS	n/a	n/a	10 mL
Total	n/a	**n/a**	**~10 mL**
Permeabilization buffer B	Stock concentration	Final concentration	Amount
TritonX-100	10% v/v	0.1% v/v	100 µL
PBS	n/a	n/a	10 mL
Total	n/a	**n/a**	**~10 mL**
Blocking buffer	Stock concentration	Final concentration	Amount
BSA	5% w/v	1% w/v	2 mL
PBS	n/a	n/a	8 mL
Total	n/a	**n/a**	**10 mL**
Washing buffer (PBST)	Stock concentration	Final concentration	Amount
Tween 20	n/a	0.05% v/v	0.5 mL
PBS	n/a	n/a	1 L
Total	n/a	**n/a**	**~1 L**

⚠ CRITICAL: Permeabilization and blocking buffers must be prepared fresh at each experiment.

Note: The washing buffer is stable at 20°C–25°C for at least one month.

STEP-BY-STEP METHOD DETAILS

Cell culture and treatment

Timing: 2–3 days

⚠ CRITICAL: Cell culture needs to be performed entirely under a Class II Biological Safety Cabinet to avoid contamination

Note: Pre-warming the complete cell culture medium and Trypsin-EDTA is recommended to avoid exposing culture cells to excessive thermal shift and minimizing detachment time, respectively.

Cells are seeded in 24-well plates containing sterile glass coverslips and allowed to attach and recover normal proliferation in view of challenging them with irradiation or other experimental conditions that may induce the accumulation of dsDNA in the cytosol.

1. Detach TS/A cells from maintenance cultures in T75 flasks
   a. Discard exhausted culture medium
   b. Add 2 mL 0.05% Trypsin-EDTA to each flask
   c. Incubate flasks for 2–3 min at 37°C

   Note: Although Trypsin-EDTA is classified as non-hazardous (NONH), it should be manipulated by wearing appropriate recommended PPE.

   Note: As detachment time can vary considerably with cell type and may be inhibited by some medium leftovers, flasks should be visually inspected for complete cell detachment before proceeding.

   Alternatives: Mechanical scraping can be employed as an alternative to enzymatic detachment.

   d. Add 7 mL complete culture medium to each flask
   e. Collect detached cells in 50 mL Falcon tubes

   Note: The amount of Trypsin-EDTA and complete culture medium employed depend on flask size. Indicatively 1 mL trypsin and 4 mL culture medium are appropriate for T25 flasks, while 5 mL trypsin and 10 mL culture medium are appropriate for T175 flasks.

   f. Centrifuge the tubes at 350 *g*, 20°C–25°C for 5 min
   g. Discard supernatants
   h. Resuspend the cell pellet in 5 mL complete culture medium

2. TS/A cells are seeded in coverslip-containing 24-well plates
   a. Count cells with a standard or automated hemocytometer
   b. Add complete culture medium to the cell suspension to achieve 1×10^4 cells/mL
   c. Seed 0.5 mL of this suspension in coverslip-containing 24-well plates and return plates to the incubator

   ⏸ Pause point: Freshly seeded cells must be allowed to attach to coverslips and resume proliferation for at least 16 h. Some cell types may require up to 24–36 h for fully recovering proliferation upon seeding.

⚠ CRITICAL: Cell density at seeding must be tailored to the overall duration of the experiment as well as the proliferation rate of each specific cell type so that control (untreated) cells achieve no more than 50%–60% confluence at fixation.

3. TS/A cells are irradiated
   a. In all wells, replace exhausted culture medium with 0.5 mL fresh, pre-warmed complete culture medium
   b. Expose cells to a single irradiation dose of 8 Gy with a SARRP

Note: Exposure time to achieve 8 Gy total dose depends on the dose-rate employed for irradiation.

Note: Any experimental treatment of choice can be tested for its ability to promote cytosolic dsDNA accumulation, provided that appropriate control conditions are implemented including (but potentially not limited to): (1) untreated or vehicle-treated cells as negative control, and (2) cells exposed to agents known for their ability to drive the release of nuclear or mitochondrial DNA in the cytosol as positive controls. The latter include irradiation (Rodriguez-Ruiz et al., 2019; Yamazaki et al., 2020) as well as a variety of pharmacological agents that interfere with DNA repair, such as poly(ADP-ribose) polymerase 1 (PARP1) (Chabanon et al., 2019; Ding et al., 2018) and ATR serine/threonine kinase (ATR) inhibitors (Dillon et al., 2017; Dillon et al., 2019).

⚠ CRITICAL: The maximal number of 24-well plates that can be simultaneously irradiated in the SARRP in the absence of a sizeable reduction in dose at the edges of the irradiation field depends on the elevation of the support platform.

Alternatives: Systems other than the SARRP can be employed for irradiation provided that they offer control on total dose (as the latter influences cytosolic dsDNA accumulation) (Vanpouille-Box et al., 2017b).

Pause point: Control and irradiated cells are maintained in standard culture conditions for the desired amount of time prior to processing for IF microscopy.

⚠ CRITICAL: The time elapsing between irradiation or other challenges and fixation may influence considerably the amount and origin of dsDNA molecules detectable in the cytosol (Harding et al., 2017; Mackenzie et al., 2017; Yamazaki et al., 2020).

Cytosolic dsDNA staining (and optionally COX4 or TFAM co-staining)

Timing: 2 days

Note: Sterile conditions are no longer required.

Note: For all steps below until staining, coverslips remain in 24-well plates.

TS/A cells are subjected to fixation and permeabilization conditions that enable for the IF microscopy-based assessment of cytosolic dsDNA molecules relative to COX4 or TFAM

4. Fixation/permeabilization
   a. Discard culture medium
   b. Fix cells with 0.5 mL of 4% paraformaldehyde (w/v in PBS) for 10 min at 20°C–25°C

Note: Optimal fixation conditions may vary with cell type.

c. Wash fixed cells twice with 0.5 mL PBS.

Pause point: Fixed cells can be stored (before staining) for up to 1 month at 4°C, provided that coverslip are covered with 1 mL PBS and that plates are sealed with parafilm to avoid PBS evaporation. In this case, coverslips should be visually inspected to ensure normal cellular morphology before resuming the protocol.

d. Transfer coverslips selected for staining to a fresh 24-well plate containing 0.5 mL PBS per well
e. Discard PBS
f. Permeabilize cells with 0.5 mL permeabilization buffer A for 10 min at 20°C–25°C

Note: Optimal permeabilization conditions may vary with cell type.

⚠ CRITICAL: Permeabilization conditions must be optimized to avoid permeabilization of intracellular membranes at this step (see troubleshooting 1).

g. Wash coverslips three times with 0.5 mL PBS
h. Block unspecific binding sites with 0.5 mL blocking buffer for 1 h 20°C–25°C

5. Primary staining
   a. Transfer coverslips sample-side onto microscopy slides or parafilm within an opaque humidified chamber containing ddH_2O

Note: Virtually any opaque or aluminum-covered container that allow for coverslips to lay in the absence of physical contact with ddH_2O can be harnessed as a humidified chamber.

Note: Up to 3 coverslips can be transferred next to each other on the same slide.

Note: It is recommended to encircle each coverslip with a hydrophobic barrier from a PAP Pen to avoid (1) an excessive dispersal of the staining solution that may allow parts of the coverslip to dry, as well as (2) cross-contamination, if different staining solutions are used for coverslips next to each other.

   b. Stain cytosolic dsDNA by gently dropping 60 µL of blocking buffer supplemented with anti-dsDNA antibodies (1:1000 v/v) onto each coverslip, and maintain coverslips in the humidified chamber for 12–16 h at 4°C
   c. Optionally, simultaneously stain COX4 or TFAM by further supplementing the blocking buffer with anti-COX4 (1:300 v/v) or anti-TFAM (1:500 v/v) antibodies

6. Secondary staining
   a. Transfer coverslips to a new 24-well plate containing 0.5 mL washing buffer per well
   b. Wash coverslips three times (5 min each) with washing buffer
   c. Stain anti-dsDNA antibodies with 0.3 mL of blocking buffer supplemented with Alexa Fluor® 594-conjugated anti-mouse antibodies (1:1000 v/v) for 30–60 min at 20°C–25°C
   d. Optionally, simultaneously stain anti-COX4 or anti-TFAM antibodies by further supplementing the blocking buffer with Alexa Fluor® 488-conjugated anti-rabbit antibodies (1:1000 v/v)

Alternatives: The staining of anti-dsDNA (and optionally anti-COX4 or anti-TFAM) antibodies can also be performed upon returning coverslips into the humidified chamber. In this case, 60 µL of blocking buffer supplemented with Alexa Fluor® 594-conjugated anti-mouse (and optionally Alexa Fluor® 488-conjugated anti-rabbit) antibodies (1:500 v/v) are used.

Alternatives: Alexa Fluor® 488-conjugated anti-mouse antibodies can be equally used for staining (30–60 min at 20°C–25°C) anti-dsDNA antibodies if no co-staining is planned. We chose to reveal dsDNA with Alexa Fluor® 594 and other structures with Alexa Fluor® 488 because with our imaging system this specific approach provided images with superior quality.

e. Wash coverslips three times (5 min each) with washing buffer

Alternatives: If coverslips were returned to the humidified chamber for the secondary staining, they must be transferred to a new 24-well plate containing 0.5 mL washing buffer per well prior to washing.

f. Wash coverslips once with 0.5 mL PBS

Alternatives: Cytosolic dsDNA and LMNB1 co-staining

Timing: 2 days

TS/A cells stained for cytosolic dsDNA molecules are further fixed, permeabilized and stained to enable the IF microscopy-based co-detection of LMNB1.

7. Fixation/permeabilization
   a. Discard PBS
   b. Re-fix cells with 0.5 mL of 4% paraformaldehyde (w/v in PBS) for 10 min at 20°C–25°C
   c. Wash coverslips three times (5 min each) with 0.5 mL PBS
   d. Re-permeabilize cells with 0.5 mL permeabilization buffer B for 10 min at 20°C–25°C

   Note: Optimal re-fixation and re-permeabilization conditions may vary with cell type.

   ⚠ CRITICAL: Additional fixation is required to obtain sharp resolution (high signal-to-noise ratio) on the dsDNA staining (see troubleshooting 2).

   e. Wash coverslips three times with 0.5 mL PBS
   f. Block unspecific binding sites with 0.5 mL blocking buffer for 1 h at 20°C–25°C

8. Primary staining
   a. Transfer coverslips sample-side onto microscopy slides or parafilm within an opaque humidified chamber containing ddH_2O.

   Note: Virtually any opaque or aluminum-covered container that allow for coverslips to lay in the absence of physical contact with ddH_2O can be harnessed as a humidified chamber.

   Note: Up to 3 coverslips can be transferred next to each other on the same slide.

   Note: It is recommended to encircle each coverslip with a hydrophobic barrier from a PAP Pen to avoid (1) an excessive dispersal of the staining solution that may allow parts of the coverslip to dry, as well as (2) cross-contamination, if different staining solutions are used for coverslips next to each other.

   b. Stain LMNB1 by gently dropping 60 μL of blocking buffer supplemented with anti-LMNB1 antibodies (1:500 v/v) onto each coverslip, and maintain coverslips in the humidified chamber for 12–16 h at 4°C

9. Secondary staining
   a. Discard the staining solution
   b. Transfer coverslip to a new 24-well plate containing 0.5 mL washing buffer per well
   c. Wash coverslips three times (5 min each) with washing buffer
   d. Stain anti-LMNB1 antibodies with 0.3 mL of blocking buffer supplemented with Alexa Fluor® 488-conjugated anti-rabbit antibodies (1:1000 v/v) for 30-60 min at 20°C–25°C

   Alternatives: The staining of anti-LMNB1 antibodies can also be performed upon returning coverslips to the humidified chamber. In this case, 60 µL of blocking buffer supplemented with Alexa Fluor® 488-conjugated anti-rabbit antibodies (1:500 v/v) are used.

   e. Wash coverslips three times (5 min each) with washing buffer

   Alternatives: If coverslips were returned to the humidified chamber for the secondary staining, they must be transferred to a new 24-well plate containing 0.5 mL washing buffer per well prior to washing

   f. Wash coverslips once with 0.5 mL PBS

Mounting and acquisition

Timing: 1–3 days

Note: The timing for mounting and acquisition is largely influenced by the number of samples, type of acquisition and number of images collected per sample.

Stained coverslips are mounted onto microscopy slides and images are acquired on confocal or widefield microscopy.

10. Mounting
    a. Place one drop of DAPI-containing mounting medium on a standard slide for microscopy

    Alternatives: Although commonly used by us and others, DAPI has broad excitation and emission spectra, which may negatively influence signal-to-noise ratio at detection wavelength employed for Alexa Fluor® 594 and Alexa Fluor® 488. As an alternative, nuclear counterstaining can be achieved by incubating coverslips in 0.3 mL Hoechst 33342 solution (working concentration 5 µg/mL in PBS) for 10 min at 20°C–25°C, followed by mounting with ProLong™ Glass Antifade Mountant (Fisher Scientific Cat #P36980)

    b. Retrieve individual coverslips from 24-well plates with Graefe forceps and rapidly dry them on paper

⚠ CRITICAL: Drying should be rapid and relatively superficial (aimed at avoiding excessive dilution of the mounting medium) as many biologically samples become auto-fluorescent if allowed to completely dry after fixation (see troubleshooting 3).

    c. Lay coverslip sample-side down on the mounting medium drop so that stained cells are in direct contact with the medium

    Note: Up to 3 coverslips can be mounted next to each other on the same slide

    d. Allow mounting medium to cure for 24 h at 20°C–25°C under protection from light

Pause point: Mounted slides can be stored at 4 °C under protection from light for at least 4 weeks in the absence of significant photobleaching prior to imaging.

11. Confocal microscopy imaging
    a. Adjust laser power and gain of each channel to satisfy the dynamic range of the experiment by imaging 2–3 control and 2–3 treated samples
    b. Once laser power and gain are selected, image at least 3 representative fields from each sample on individual blue (DAPI), red (cytosolic dsDNA) and green (LMNB1, COX4 or TFAM) channels (see above for excitation/emission peaks and laserline/detector settings)
    c. Single-channel images of specific Z-planes can be merged, and/or single-channel or merge images can be reconstructed into 3D animations (based on the maximum projection approach) for visualization purposes

⚠ CRITICAL: Laser power and gain should be adjusted to prevent overexposure of each fluorophore even in the brightest condition.

Note: All commercial confocal microscopes are provided with software packages that enable merging and 3D reconstructions.

Alternatives: ImageJ/FIJI (NIH) can also be employed for merging and 3D reconstruction, respectively.

12. Widefield microscopy imaging
    a. Adjust illumination power and exposure time of each channel to satisfy the dynamic range of the experiment by imaging 2–3 control and 2–3 treated samples
    b. Once illumination power and exposure time are selected, image at least 3 fields per coverslip on individual blue (DAPI), red (cytosolic dsDNA) and green (LMNB1, COX4 or TFAM) channels (see above for excitation/emission peaks and laserline/detector settings)
    c. Single-channel images can be merged for visualization purposes and/or subjected to automated analysis for quantitative assessments, as detailed below

⚠ CRITICAL: Illumination power and exposure time should be adjusted to prevent overexposure of each fluorophore even in the brightest condition.

Note: ImageJ/FIJI and widefield microscope software packages for acquisition can be used to merge images.

Pause point: Images can be stored indefinitely prior to analysis.

Automated image analysis

Timing: 1 day

Single-channel widefield microscopy images are processed for the assessment of number of cytosolic dsDNA-positive foci in each cell, percentage of cells containing cytosolic dsDNA-positive foci (Figure 1), and spatial localization of cytosolic dsDNA-positive foci with respect to COX4, TFAM or LMNB1.

Note: Photoshop (Adobe), ImageJ/FIJI or equivalent imaging software is employed to adjust images prior to automated analysis.

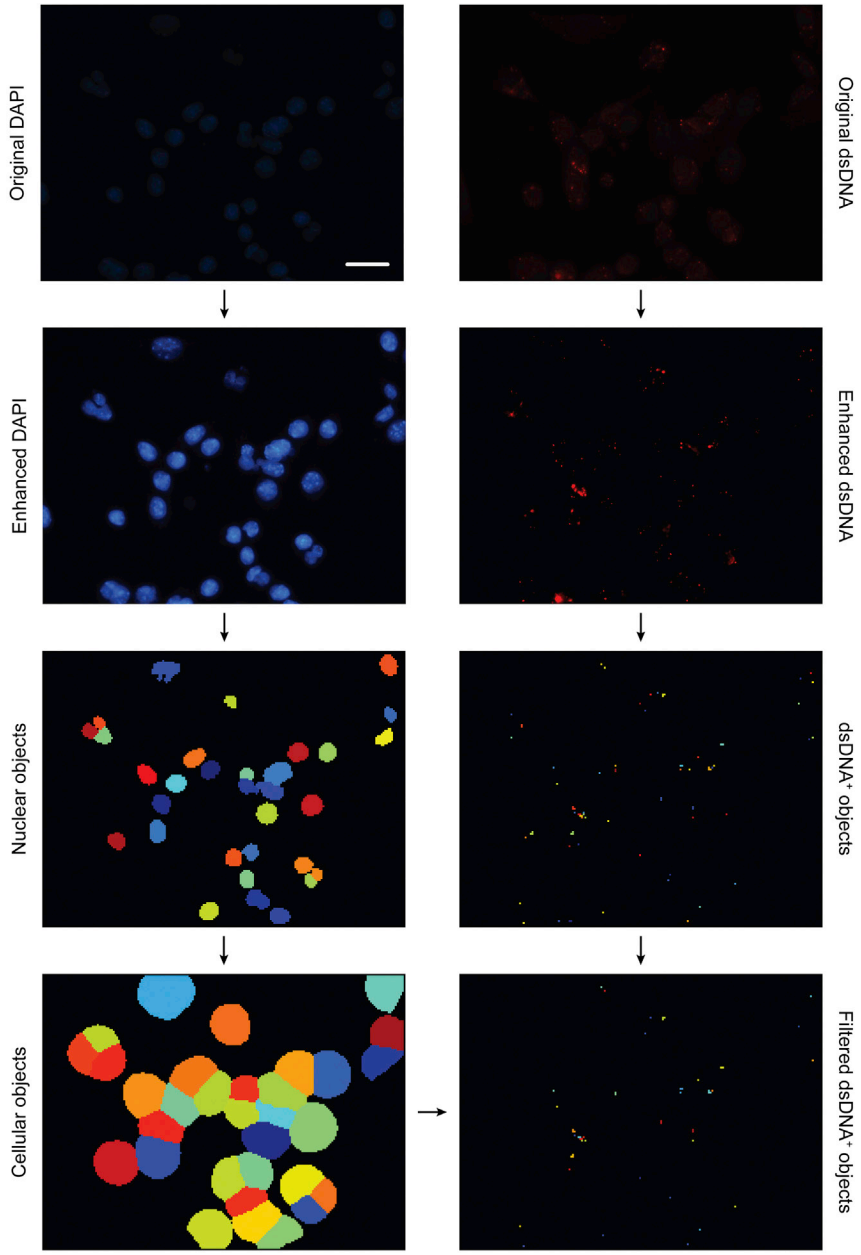

Figure 1. Pipeline for automated image analysis

Images that exemplify automated segmentation and quantification of cytosolic dsDNA^{+} objects. Scale bar = 30 μm.

13. Generation of LUT files
    a. Open single-channel images from multiple conditions and adjust levels manually to obtain sharp resolution. Carefully avoid over- and under-exposure by monitoring histograms.
    b. Use the function "Save presets" in the Levels pop-up window to save "Look Up Table" (LUT) files for each channel
    c. Apply LUT files as defined above to each single-channel image by the function "Load presets" in the Levels pop-up window

d. Save level-optimized single-channel images in a dedicated folder for automated image analysis

Alternatives: Cell Profiler can be employed to adjust single-channel images prior to automated image analysis (Kamentsky et al., 2011). This is expected to shorten workflow, but requires implementation of additional steps not described herein.

Note: Adjusting the levels in Photoshop could alter pixel intensities and scaling of the grey values of the image and hence influence intensity measurements. That said, comparing the results of automated image analysis to quantifications by three independent operators, we never found this potential issue to significantly alter quantitative assessments.

Note: Cell Profiler is employed for automated image analysis based on publicly available algorithms that have been customized to fit the identification of nuclear and cytosolic objects (Kamentsky et al., 2011).

Note: Before running the actual analysis, it is recommended to test each step using the "Test Mode".

14. Identification of nuclear and cytosolic objects with Cell Profiler
    a. Identification of nuclear objects
        i. Identify nuclear objects as objects of 40–110 pixels diameter in blue-channel images with the "IdentifyPrimaryObjects" package

Alternatives: In case of LMNB1 co-staining, green-channel images can be equally employed to define nuclear objects as above.

        ii. Discard objects outside this diameter range as well as objects on the image borders
        iii. Identify clumped objects by "Shape" and separate them based on "Signal intensity". Turn on the following additional features "Automatically calculate size of the smoothing filter for declumping" and "Automatically calculate minimal allowed distance between local maxima".
    b. Identification of cytoplasmic areas
        i. On blue-channel images with identified nuclear objects that are used as input objects, identify cellular objects with the "IdentifySecondaryObjects" package, by the distance - N method expanding the primary object by 50 pixels
        ii. Using the package "IdentifyTertiaryObjects", define cytoplasmic areas subtractively based on cellular and nuclear objects

Note: The optimal extent and method of expansion to identify cellular objects may vary considerably with cell type and magnification. Visual comparison of cytoplasmic areas in processed images vs. cells in enhanced green-channel images can be used to assess fidelity and alter the extent of expansion if needed.

Alternatives: In case of LMNB1 co-staining, green-channel images can be equally employed to define cytoplasmic areas as above.

15. Identification of dsDNA$^+$, COX4$^+$ and TFAM$^+$ objects with Cell Profiler
    a. Use the he "EnhanceOrSuppressFeatures" package to enhance speckles of 15 pixels diameter on red- or green-channel images, depending on the secondary antibodies employed for IF

Note: The optimal diameter for this step may vary considerably with cell type and magnification.

⚠ CRITICAL: Insufficient or excessive enhancement largely compromises automated image analysis as it prevents proper identification of prevents correct identification of primary objects and hence precise quantitative assessments (see troubleshooting 5).

b. On enhanced images, identify dsDNA$^+$, COX4$^+$ or TFAM$^+$ objects as objects of 4–25 pixels diameter on red- or green-channel images, depending on the secondary antibodies employed for IF, with the "IdentifyPrimaryObjects" package
c. Discard objects outside this diameter range as well as objects on the image borders
d. Identify clumped objects by "Shape" and separate them based on "Signal intensity". Turn on the following additional features "Automatically calculate size of the smoothing filter for declumping" and "Automatically calculate minimal allowed distance between local maxima"
e. Apply the "MeasureObjectIntensity" package to dsDNA$^+$, COX4$^+$ or TFAM+ objects
f. Discard objects with signal intensity <0.04

Note: Intensity, size thresholds and declumping parameters for defining and discarding dsDNA$^+$, COX4$^+$ and TFAM$^+$ objects may vary in different cell types, across experiments and/or with different image acquisition devices. Visual comparison of dsDNA$^+$, COX4$^+$ and TFAM$^+$ objects in enhanced images vs. dsDNA$^+$, COX4$^+$ and TFAM$^+$ structured in enhanced red- or green-channel images can be used to assess fidelity and alter parameters if needed.

Note: The optical resolution of our system (~0.32 μm) is intrinsically insufficient to resolve cytosolic dsDNA$^+$ foci closer to each other of <0.32 μm, implying that quantitative results will suffer from some degree of underestimation, especially in presence of cytosolic dsDNA$^+$ foci at high density.

16. Identification of cytosolic dsDNA$^+$ objects with Cell Profiler
    a. Relate dsDNA$^+$ objects and cytoplasmic areas (defined as above) as child and parent, respectively, with the "RelateObjects" package
    b. Using the "FilterObjects" package, select cytoplasmic areas containing a minimum value of 1 children object as positive cells.

Note: Thresholds should be validated for each set of images as they might vary in different cell types, across experiments and/or with different image acquisition devices. "Test mode" should be used to validate that the parameters are adequate for each set of images. Specifically, the value of children objects employed to define positive cells is selected as the closest integer number below to the average number of cytosolic dsDNA$^+$ dots observed in untreated cells (in our settings, 1.46 see Table 1)

Optional: Quantitative results and images exemplifying the analytic pathway can be exported in multiple file formats

    c. Interrogate quantitative data for number of cytosolic dsDNA$^+$ dots per cell and percentage of cells exhibiting cytosolic dsDNA$^+$ dots.

17. Colocalization with Cell Profiler
    a. Nuclear dsDNA$^+$ objects
        i. Relate dsDNA$^+$ objects and nuclear objects (defined as above) as parent and child, respectively, with the "RelateObjects" package
        ii. Using the "FilterObjects" package, identify filtered dsDNA objects as nuclear by children category and nuclear count with a minimum value of 1

Table 1. Example of automated image analysis output

Sample	Field	Condition	Cytosolic dsDNA$^+$ foci per positive cell (mean)	% of cells with > 1 cytosolic dsDNA$^+$ foci	% of dsDNA$^+$ foci overlapping with COX4 signal	% of dsDNA$^+$ foci overlapping with TFAM signal	% of dsDNA$^+$ foci overlapping with LMNB1 signal
1	1	Control	1.33	31.82	N/A	N/A	N/A
1	2	Control	1.52	37.31	N/A	N/A	N/A
1	3	Control	1.33	30.00	N/A	N/A	N/A
2	1	Control	1.89	25.35	N/A	N/A	N/A
2	2	Control	1.36	36.67	N/A	N/A	N/A
2	3	Control	1.35	34.33	N/A	N/A	N/A
		Mean	1.46	32.58	N/A	N/A	N/A
		SEM	0.09	1.84	N/A	N/A	N/A
		SD	0.20	4.12	N/A	N/A	N/A
7	1	RT	2.44	56.25	N/A	N/A	27.27
7	2	RT	2.30	74.07	N/A	N/A	30.43
7	3	RT	2.38	70.00	N/A	N/A	30.00
8	1	RT	3.44	57.14	N/A	N/A	23.64
8	2	RT	3.47	68.18	N/A	N/A	23.08
8	3	RT	3.15	60.61	N/A	N/A	20.63
9	1	RT	3.32	67.86	91.89	N/A	N/A
9	2	RT	4.11	75.00	80.00	N/A	N/A
9	3	RT	3.78	64.29	91.67	N/A	N/A
10	1	RT	8.00	75.00	94.44	N/A	N/A
10	2	RT	2.46	68.42	87.50	N/A	N/A
10	3	RT	6.18	73.33	96.00	N/A	N/A
11	1	RT	2.08	50.00	N/A	92.59	N/A
11	2	RT	2.11	42.86	N/A	72.00	N/A
11	3	RT	2.71	77.78	N/A	73.53	N/A
12	1	RT	2.57	50.00	N/A	87.50	N/A
12	2	RT	4.80	62.50	N/A	75.86	N/A
12	3	RT	2.00	50.00	N/A	72.73	N/A
		Mean	3.57	64.26	90.25	79.04	25.84
		SEM	0.51	3.08	2.37	3.58	1.63
		SD	1.53	10.16	5.29	9.01	3.65
		p value	*p =0.0071	*p < 0.001	#p < 0.001	#p < 0.001	#p < 0.001

See also Figure 3.

*Unpaired t test, as compared to untreated TS/A cells;

#Fisher's exact test, as compared to 50%–50% random distribution.

Optional: Quantitative results and images exemplifying the analytic pathway can be exported in multiple file formats

iii. Interrogate quantitative data for percentage of dsDNA$^+$ objects co-localizing with nuclear (DAPI$^+$ or LMNB1$^+$) objects over total dsDNA$^+$ objects

b. dsDNA:COX4 or dsDNA:TFAM co-localization

i. Relate dsDNA$^+$ objects and COX4$^+$ or TFAM$^+$ objects (defined as above) as child and parent, respectively, with the "RelateObjects" package

ii. Using the "FilterObjects" package, filter results using 1 as a minimum measurement value (COX4$^+$ or TFAM$^+$ objects that do not co-localize with dsDNA$^+$ objects are excluded from further analysis)

Optional: Quantitative results and images exemplifying the analytic pathway can be exported in multiple file formats

iii. Interrogate quantitative data for percentage of dsDNA$^+$ objects co-localizing with COX4$^+$ or TFAM$^+$ objects over total dsDNA$^+$ objects

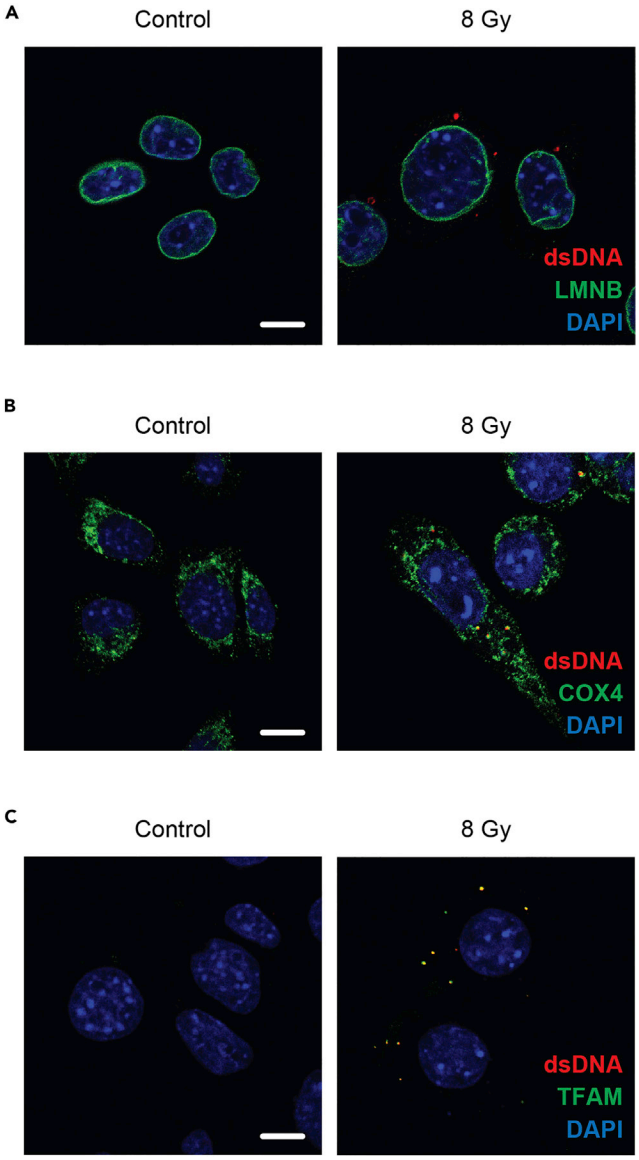

Figure 2. Confocal microscopy-based assessment of cytosolic dsDNA relative to LMNB1$^+$ nuclear structures, COX4$^+$ mitochondrial structures and TFAM

(A–C). Wild-type mouse mammary adenocarcinoma TS/A cells were maintained in control conditions or subjected to γ irradiation (8 Gy) and cultured in control conditions for 24 h, then stained with DAPI (blue nuclear counterstain, A–C) plus dsDNA-specific (red, A–C) and LMNB1-specific (green, A), COX4-specific (green, B) or TFAM-specific (green, C) antibodies and processed for confocal microscopy. Scale bar = 10 μm. See also Methods videos S1, S2, S3, S4, S5, and S6.

Pause point: Automated analysis can be paused indefinitely at any of the steps above.

EXPECTED OUTCOMES

Confocal images of TS/A cells exposed to a single radiation therapy (RT) fraction of 8 Gy and 24 h later processed as described above reveal the accumulation of cytosolic foci staining positively for dsDNA that are for the most part distant from LMNB1$^+$ nuclear structures (Figure 2A and Methods videos S1 and S2) but in the proximity of COX4$^+$ mitochondrial structures (Figure 2B and Methods videos S3 and S4) and co-localize with TFAM (Figure 2C and Methods videos S5 and S6). This is in line with the notion that RT drives MOMP permeabilization linked to the exposure of mtDNA to

the cytosol (Yamazaki et al., 2020). Importantly, the cytosolic dsDNA$^+$ foci accumulating in irradiated TS/A cells often do not appear precisely co-localize with COX4$^+$ mitochondria, but reside in their close proximity (Figure 2B and Methods videos S3 and S4), which reflects the ability of some mtDNA molecules to bulge into the cytosol through permeabilized mitochondrial membranes (McArthur et al., 2018). Optical aberration is excluded as a possible technical determinant for this observation as cytosolic dsDNA$^+$ dots revealed with Alexa Fluor® 594 precisely co-localize with TFAM when the latter is revealed with Alexa Fluor® 488 (the same fluorophore used for COX4, to which instead cytosolic dsDNA$^+$ dots do not precisely co-localize) (Figure 2C and Methods videos S5 and S6).

Widefield microscopy images of TS/A cells exposed to a single RT fraction of 8 Gy and 24 h later processed as described above, reveal that the accumulation of average 3.57 cytosolic foci staining positively for dsDNA per dsDNA$^+$ cell, with average 64.26% cells exhibiting more than 1 cytosolic dsDNA-positive foci (Figure 3A and Table 1). Of these foci, approximately 25% are expected to localize in the proximity of LMNB1$^+$ nuclear structures (Figure 3B and Table 1), 90% are expected to reside near COX4$^+$ mitochondria (Figure 3C and Table 1), and 79% are expected to co-localize with TFAM (Figure 3D and Table 1).

Importantly, not only cell type, but also (1) RT dose and fractionation schedule, and (2) time elapsing between RT and fixation are expected to considerably affect these values, as lower RT dose and prolonged post-RT culture are associated with limited MOMP coupled with increased micronucleation as a consequence of mitotic catastrophe (Harding et al., 2017; Vitale et al., 2011). In this setting, an increased proportion of cytosolic dsDNA is expected to originate from nuclear DNA and hence preferentially localize in the proximity of LMNB1$^+$ nuclear structures.

QUANTIFICATION AND STATISTICAL ANALYSIS

Quantitative results obtained upon automated image analysis as detailed above are processed as follows. Cytosolic dsDNA data are quantified as mean dsDNA$^+$ dots per positive cell or percentage of positive cells (containing at least 1 dsDNA$^+$ dot) in each image. Co-localization is quantified as percentage of dsDNA$^+$ foci with overlapping COX4, TFAM or LMNB1 signal in each image. A minimum of 3 fields from a total of at least 2 biologically independent samples collected over a minimum of 2 independent experiments (6 data points, n = 2) ensures statistical validity. Especially for particularly heterogeneous cell populations, however, we recommend to analyze at least 3 fields from a total of at least 3 biologically independent samples collected over a minimum of 2 independent experiments (9 data points, n = 3). Data can be represented as means $\pm$ SEM (assessing how far the sample mean is likely to be from the true population mean) or means $\pm$ SD (assessing the dispersion of individual data values as compared to the mean). Statistical significance for dsDNA$^+$ dots per positive cell or percentage of positive cells is assessed with unpaired t test. Statistical significance for co-localization is assessed with Fisher's exact test (as compared to a 50%–50% random distribution).

LIMITATIONS

The major limitation of this protocol is that it requires very strict permeabilization conditions, implying that: (1) the technique cannot be applied to bioptic samples, which are normally available as formalin-fixed paraffin-embedded (FFPE) or fresh-frozen material; and that (2) permeabilization conditions may require further optimization to initially achieve plasma, but not nuclear and inner mitochondrial, membrane permeabilization in specific cell types. Moreover, although possible in principle, we are unaware of this technique being successfully applied to fresh tissue sections, and considerable variations from the protocol described above may be required to obtain reliable and reproducible results. Additional constraints reflect the global setup and aims of the technique. Specifically, this method is not intended (and hence unsuitable) to detect/quantify dsDNA molecules within intracellular membranous compartments such as the nucleus, mitochondria or endosomes/

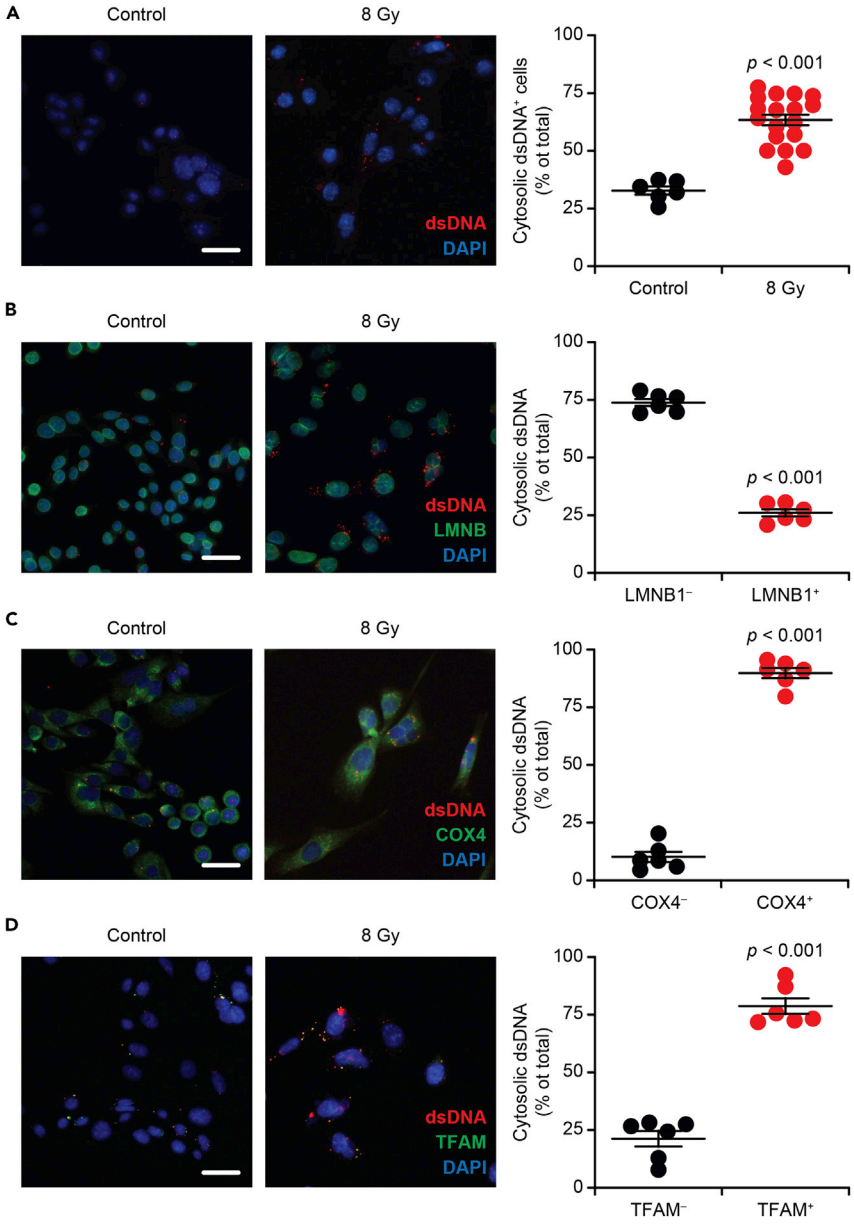

Figure 3. Widefield microscopy-based quantification of cytosolic dsDNA$^+$ foci relative to LMNB1$^+$ nuclear structures, COX4$^+$ mitochondrial structures and TFAM

(A–D). Wild-type mouse mammary adenocarcinoma TS/A cells were maintained in control conditions or subjected to γ irradiation (8 Gy) and cultured in control conditions for 24 h, then stained with DAPI (blue nuclear counterstain, A–D) plus dsDNA-specific (red, A–D) and LMNB1-specific (green, B), COX4-specific (green, C) or TFAM-specific (green, D) antibodies and processed for widefield microscopy. Representative images and quantitative data are reported. Scale bar = 30 μm. Results are means ± SEM plus individual data points based on 6-18 images from 2 biologically independent samples over 2 independent experiments. *p* values are reported, as obtained by unpaired t test(**A**) or Fisher's exact test, as compared to 50%-50% random distribution (B). See also Table 1.

lysosomes. Along similar lines, dsDNA molecules from intracellular parasites (be them prokaryotic or eukaryotic, including *Mycoplasma spp.*) cannot be detected with this technique, unless the content of such parasites has been released in the cytosol upon cell death (and hence dsDNA is no longer secluded within the parasite plasma membrane). Conversely, we expect this protocol to enable

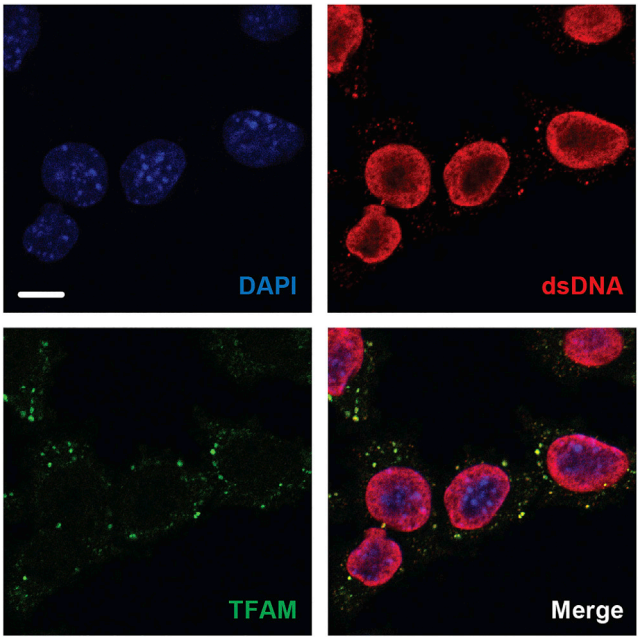

Figure 4. Confocal microscopy-based assessment of cytosolic dsDNA relative to TFAM upon excessive permeabilization

Wild-type mouse mammary adenocarcinoma TS/A cells were maintained in control conditions then subjected to strong permeabilization with 0.1% TritonX-100 for 10 min, stained with DAPI (blue nuclear counterstain) plus dsDNA-specific (red) and TFAM-specific (green) antibodies and processed for confocal microscopy. Scale bar = 10 μm. See also Methods video S7.

the detection/quantification of viral dsDNA molecules in eukaryotic cells infected by viral species that harness dsDNA as repository of genetic information or as a lytic cycle intermediate, provided that such dsDNA molecules obtain physical access to the cytosol prior to entering the nucleus or being packaged into newly formed virions (Jones et al., 2020).

TROUBLESHOOTING

Problem 1

Excessive permeabilization for dsDNA staining (step 4)

When excessively harsh or prolonged permeabilization conditions are applied before dsDNA staining, most/all intracellular membranes become permissive for access by primary and secondary antibodies, resulting in the labeling of nuclear, mitochondrial and potentially endosomal/lysosomal dsDNA molecules, as well as intramitochondrial TFAM (Figure 4).

Potential solution

Milder permeabilization conditions must be employed, either by altering the composition of the permeabilization reagent or by decreasing fixation/permeabilization time.

Problem 2

Insufficient fixation before LMNB1 staining (step 7)

When LMNB1 staining is not preceded by fixation, or when fixation prior to co-staining is excessively mild, the dsDNA signal-to-background ratio is reduced, potentially compromising automated image analysis upon widefield microscopy (Figure 5).

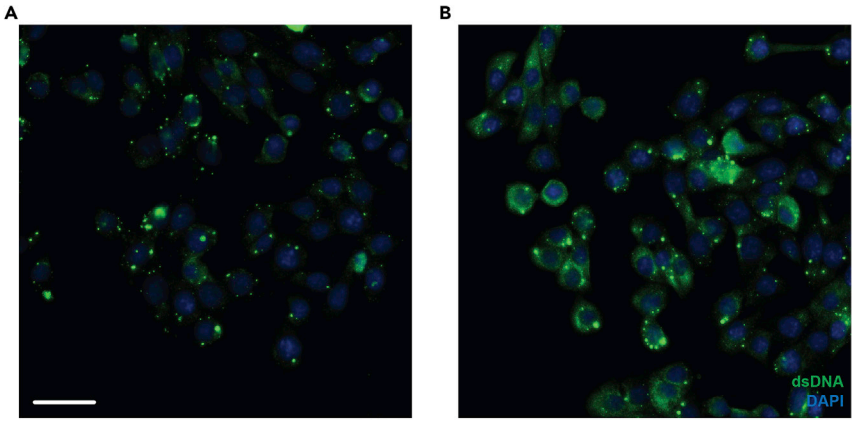

Figure 5. Widefield microscopy-based assessment of cytosolic dsDNA relative to an additional marker in the absence of fixation prior to LMNB1 staining

Wild-type mouse mammary adenocarcinoma TS/A cells were exposed to γ irradiation (8 Gy) and cultured in control conditions for 24 h, then stained with DAPI (blue nuclear counterstain) plus dsDNA-specific (green) in the context (A) or not (B) of fixation prior to LMNB1 staining, and processed for widefield microscopy. Scale bar = 30 μm.

Potential solution

Further fixation must be performed prior to co-staining. If dsDNA signal-to-background ratios appear suboptimal, stronger fixation conditions must be employed, either by altering the composition of the fixation reagent or by increasing fixation time.

Problem 3

Limited signal-to-noise ratio (step 10)

If coverslips are excessively dried prior to mounting, cells may become highly auto-fluorescent, resulting in limited signal-to-noise ratio at various detection wavelengths.

Potential solution

Drying must be rapid and incomplete, strictly aimed at removing PBS drops that may dilute the mounting medium and potentially reduce its adhesiveness.

Problem 4

Incorrect nuclear object identification (step 14)

Using an incorrect size to identify nuclear objects compromises the precise identification of both cellular objects and cytoplasmic areas (Figure 6A).

Potential solution

Identification of nuclear objects must be visually verified prior to initiation of automated analysis. Size must be adapted until satisfactory identification is achieved on a few test images. The "Watershed" function may also be employed to improve the detection of nuclear objects.

Problem 5

Excessive/insufficient signal enhancement (step 15)

Signal enhancement can be achieved by a variety of approaches that may not necessarily return optimal results, depending on various features of the signal and input image. Excessive or insufficient enhancement are common problems (Figure 6B).

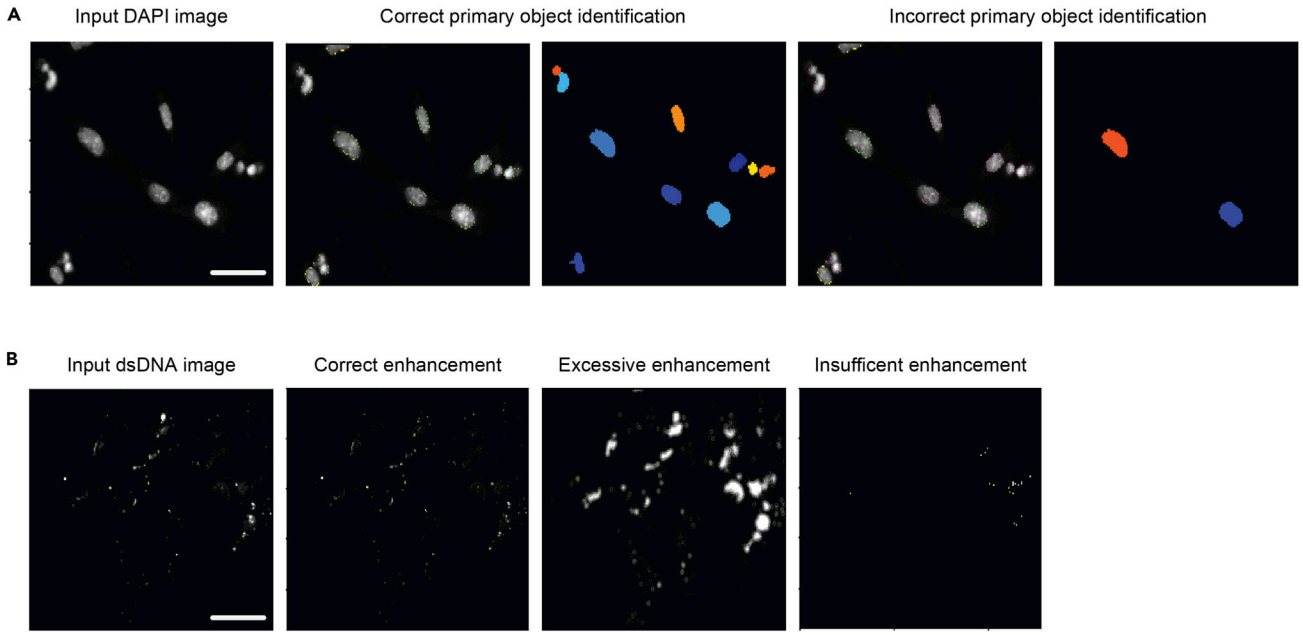

Figure 6. Common issues with automated image analysis

(A and B). Representative widefield images of wild-type mouse mammary adenocarcinoma TS/A cells maintained in control conditions processed to highlight potential issues with the identification of nuclear objects (A) or signal enhancement (B). Scale bar = 30 μm.

Potential solution

Enhancement must be visually verified prior to initiation of automated analysis. Alternative enhancement techniques or parameters must be tested until satisfactory enhancement is achieved on a few test images.

RESOURCE AVAILABILITY

Lead contact

Further information and requests for resources and reagents should be directed to and will be fulfilled by the lead contact, Lorenzo Galluzzi (deadoc80@gmail.com).

Materials availability

This study did not generate new unique reagents.

Data and code availability

Source data for Figure 3 is presented in Table 1. Original images for qualitative and quantitative assessments that have not been included in the present article are available upon reasonable request to the lead contact, Lorenzo Galluzzi (deadoc80@gmail.com). This study did not generate new code.

SUPPLEMENTAL INFORMATION

Supplemental information can be found online at https://doi.org/10.1016/j.xpro.2021.100488.

ACKNOWLEDGMENTS

We are indebted to Jeffrey Kraynak from the WCM Radiation Biology Core Facility (established with support from an NIH/NCI Small Instrumentation Grant to Dr. Formenti, #S10-RR027619-01) for help with irradiation procedures. The LG lab is supported by a Breakthrough Level 2 grant from the US Department of Defense (DoD), Breast Cancer Research Program (BRCP) (#BC180476P1), by the 2019 Laura Ziskin Prize in Translational Research (#ZP-6177, PI: Formenti) from the Stand Up to Cancer (SU2C), by a Mantle Cell Lymphoma Research Initiative (MCL-RI, PI: Chen-Kiang) grant from the

Leukemia and Lymphoma Society (LLS), by a startup grant from the Department of Radiation Oncology at Weill Cornell Medicine (New York, US), by a Rapid Response grant from the Functional Genomics Initiative (New York, US), by industrial collaborations with Lytix (Oslo, Norway) and Phosplatin (New York, US), and by donations from Phosplatin (New York, US), the Luke Heller TECPR2 Foundation (Boston, US), and SOTIO a.s. (Prague, Czech Republic).

AUTHOR CONTRIBUTIONS

A.S. optimized the technique with input from T.Y., N.B., and G.P., acquired immunofluorescence microscopy images, and generated 3D reconstructions. T.Y. generated biological samples for processing by A.S. A.B. developed the automated pipeline for image processing and quantification. A.B., N.B., and G.P. prepared display items. L.G. supervised all aspects of the study and wrote the manuscript with input from A.S., T.Y., and A.B. All authors agree with the final version of the article.

DECLARATION OF INTERESTS

L.G. reports receiving research funding from Lytix and Phosplatin (completed) and consulting/advisory honoraria from Boehringer Ingelheim, AstraZeneca, OmniSeq, The Longevity Labs, Inzen, Onxeo, and the Luke Heller TECPR2 Foundation.

REFERENCES

Chabanon, R.M., Muirhead, G., Krastev, D.B., Adam, J., Morel, D., Garrido, M., Lamb, A., Henon, C., Dorvault, N., Rouanne, M., et al. (2019). PARP inhibition enhances tumor cell-intrinsic immunity in ERCC1-deficient non-small cell lung cancer. J. Clin. Invest. *129*, 1211–1228.

De Giovanni, C., Nicoletti, G., Landuzzi, L., Palladini, A., Lollini, P.L., and Nanni, P. (2019). Bioprofiling TS/A murine mammary cancer for a functional precision experimental model. Cancers (Basel) *11*.

Dillon, M.T., Barker, H.E., Pedersen, M., Hafsi, H., Bhide, S.A., Newbold, K.L., Nutting, C.M., McLaughlin, M., and Harrington, K.J. (2017). Radiosensitization by the ATR Inhibitor AZD6738 through generation of acentric micronuclei. Mol. Cancer Ther. *16*, 25–34.

Dillon, M.T., Bergerhoff, K.F., Pedersen, M., Whittock, H., Crespo-Rodriguez, E., Patin, E.C., Pearson, A., Smith, H.G., Paget, J.T.E., Patel, R.R., et al. (2019). ATR inhibition potentiates the radiation-induced inflammatory tumor microenvironment. Clin. Cancer Res. *25*, 3392–3403.

Ding, L., Kim, H.J., Wang, Q., Kearns, M., Jiang, T., Ohlson, C.E., Li, B.B., Xie, S., Liu, J.F., Stover, E.H., et al. (2018). PARP inhibition elicits STING-dependent antitumor immunity in brca1-deficient ovarian cancer. Cell Rep. *25*, 2972–2980 e2975.

Han, Y., Chen, L., Liu, H., Jin, Z., Wu, Y., Wu, Y., Li, W., Ying, S., Chen, Z., Shen, H., and Yan, F. (2020). Airway epithelial cGAS is critical for induction of experimental allergic airway inflammation. J. Immunol. *204*, 1437–1447.

Harding, S.M., Benci, J.L., Irianto, J., Discher, D.E., Minn, A.J., and Greenberg, R.A. (2017). Mitotic progression following DNA damage enables pattern recognition within micronuclei. Nature *548*, 466–470.

Jones, J.E., Le Sage, V., and Lakdawala, S.S. (2020). Viral and host heterogeneity and their effects on the viral life cycle. Nat. Rev. Microbiol. *19*, 272–282.

Kamentsky, L., Jones, T.R., Fraser, A., Bray, M.A., Logan, D.J., Madden, K.L., Ljosa, V., Rueden, C., Eliceiri, K.W., and Carpenter, A.E. (2011). Improved structure, function and compatibility for CellProfiler: modular high-throughput image analysis software. Bioinformatics *27*, 1179–1180.

Lam, A.R., Bert, N.L., Ho, S.S., Shen, Y.J., Tang, L.F., Xiong, G.M., Croxford, J.L., Koo, C.X., Ishii, K.J., Akira, S., et al. (2014). RAE1 ligands for the NKG2D receptor are regulated by STING-dependent DNA sensor pathways in lymphoma. Cancer Res. *74*, 2193–2203.

Mackenzie, K.J., Carroll, P., Martin, C.A., Murina, O., Fluteau, A., Simpson, D.J., Olova, N., Sutcliffe, H., Rainger, J.K., Leitch, A., et al. (2017). cGAS surveillance of micronuclei links genome instability to innate immunity. Nature *548*, 461–465.

McArthur, K., Whitehead, L.W., Heddleston, J.M., Li, L., Padman, B.S., Oorschot, V., Geoghegan, N.D., Chappaz, S., Davidson, S., San Chin, H., et al. (2018). BAK/BAX macropores facilitate mitochondrial herniation and mtDNA efflux during apoptosis. Science *359*, eaao6047.

Rodriguez-Ruiz, M.E., Buque, A., Hensler, M., Chen, J., Bloy, N., Petroni, G., Sato, A., Yamazaki, T., Fucikova, J., and Galluzzi, L. (2019). Apoptotic caspases inhibit abscopal responses to radiation and identify a new prognostic biomarker for breast cancer patients. Oncoimmunology *8*, e1655964.

Rodriguez-Ruiz, M.E., Vitale, I., Harrington, K.J., Melero, I., and Galluzzi, L. (2020). Immunological impact of cell death signaling driven by radiation on the tumor microenvironment. Nat. Immunol. *21*, 120–134.

Shen, Y.J., Le Bert, N., Chitre, A.A., Koo, C.X., Nga, X.H., Ho, S.S., Khatoo, M., Tan, N.Y., Ishii, K.J., and Gasser, S. (2015). Genome-derived cytosolic DNA mediates type I interferon-dependent rejection of B cell lymphoma cells. Cell Rep. *11*, 460–473.

Vanpouille-Box, C., Alard, A., Aryankalayil, M.J., Sarfraz, Y., Diamond, J.M., Schneider, R.J., Inghirami, G., Coleman, C.N., Formenti, S.C., and Demaria, S. (2017a). DNA exonuclease Trex1 regulates radiotherapy-induced tumour immunogenicity. Nat. Commun. *8*, 15618.

Vanpouille-Box, C., Formenti, S.C., and Demaria, S. (2017b). TREX1 dictates the immune fate of irradiated cancer cells. Oncoimmunology *6*, e1339857.

Vanpouille-Box, C., Hoffmann, J.A., and Galluzzi, L. (2019). Pharmacological modulation of nucleic acid sensors - therapeutic potential and persisting obstacles. Nat. Rev. Drug Discov. *18*, 845–867.

Vitale, I., Galluzzi, L., Castedo, M., and Kroemer, G. (2011). Mitotic catastrophe: a mechanism for avoiding genomic instability. Nat. Rev. Mol. Cell Biol. *12*, 385–392.

Yamazaki, T., Kirchmair, A., Sato, A., Buque, A., Rybstein, M., Petroni, G., Bloy, N., Finotello, F., Stafford, L., Navarro Manzano, E., et al. (2020). Mitochondrial DNA drives abscopal responses to radiation that are inhibited by autophagy. Nat. Immunol. *21*, 1160–1171.